

A facile method to prepare UV light-triggered self-healing polyphosphazenes

Lei Hu · Xinjian Cheng · Aiqing Zhang

Received: 20 October 2014 / Accepted: 12 December 2014 / Published online: 24 December 2014
© Springer Science+Business Media New York 2014

Abstract It is of importance to prepare self-healing materials using reversible covalent bonding within polymers. In this work, we introduced ethyl 4-aminocinnamate (EA) to polyphosphazenes to prepare a novel self-healing elastomer via the reversible photochemical [2+2] cycloaddition. Linear polymer, poly[(*n*-butylamino)_x(ethyl 4-aminocinnamate)_y] phosphazene, was synthesized firstly via the ring-opening polymerization, and then substitution reaction was conducted to introduce EA as side groups. Consequently, the damaged polyphosphazenes were re-healed by being exposed to UV light. Their structures were characterized by ¹H-NMR, ³¹P-NMR, FTIR, and GPC; thermal properties were tested by TGA and DMA. The [2+2] cycloaddition reaction and retro-[2+2] cycloaddition were investigated by UV-vis. The results showed that the broken polyphosphazenes could be self-healed by the UV light irradiation at 365 nm. The damaged polyphosphazene could be re-healed almost completely within about half an hour.

Introduction

Self-healing polymers have remarkable functional structures. One of the most outstanding characteristics is their

ability of self-repairing and renewing independently or automatically [1–3]. In recent years, engineering materials, especially polymers, have been applied to almost all aspects of personal life and industry. However, microcracks in the polymer structure caused by constant or cyclic stress fatigue and scratches on surface tremendously reduced the working life of the polymers [4]. In order to heal the damages and prolong the lifespan of the polymeric materials, smart self-healing systems have been concerned and developed to polymer structures [5].

Numerous literatures reported a series of self-healable polymers using the embedded microcapsules and pipelines [6]. Briefly, to achieve quick self-healing, the adhesion of liquid healing agent in the embedded microcapsules/pipelines was utilized [1, 7–9]. Soo et al. [10] have reported a new, chemically stable self-healing materials system using the tin-catalyzed polycondensation of phase-separated droplets containing hydroxyl end-functionalized polydimethylsiloxane and polydiethoxysiloxane. The catalyst, di-*n*-butyltin dilaurate, is encapsulated in polyurethane microcapsules. And the microcapsules were embedded in a vinyl ester matrix and released when the capsules are broken. These healing reagents possessed some advantages over the previous self-healing methodology, including the healing chemistry, i.e., they remain stable in humid or wet environments and they are stable at an elevated temperature (>100 °C). Xiao et al. [11] carried out a two-component healing system based on epoxy monomer and (C₂H₅)₂O·BF₃. Curing of the epoxy spreads out quickly so long as the epoxy liquid contacts (C₂H₅)₂O·BF₃ because the reaction between epoxy and BF₃ is an active cationic chain polymerization. Also, the novel method was proposed to protect (C₂H₅)₂O·BF₃ from being damped via being absorbed by porous carriers, short sisal fibers, and then coated by polystyrene as a shield. Although, this

Xinjian Cheng is the joint first author.

L. Hu · X. Cheng
College of Textiles and Garments, Southwest University,
Chongqing 400715, People's Republic of China

L. Hu · X. Cheng (✉) · A. Zhang
School of Chemistry and Materials Science, South-Central
University for Nationalities, Wuhan 430074, People's Republic
of China
e-mail: chxj606@163.com

method to prepare self-repairing system was common and most studied, there were some limitations such as the restricted availability of the solid-phase catalyst and the exhaust of the healing agent which became depleted upon repeated healing of the same crack [12, 13].

The self-healing with reversible intermolecular interaction includes supermolecular interaction, and covalent bonds, however, successfully break through this limit, which could heal the same crack many times [14–16]. For example, a recent study by Zeng et al. [17] reported a supramolecular polymer gel formed between triptycene-based bis(crown ether) and copolymer containing dibenzylammonium (DBA) moieties by host–guest interactions. This supramolecular polymer gel showed multi-stimuli reversible responsiveness, such as thermo-, acid/base-, and chemo-induced gel–sol transitions. The result of rheological measurements showed that the gel has an intrinsic self-healing property, and the process could be repeated at least three times. In our previous work [18], novel cross-linked polyphosphazenes with remendable capacity have been synthesized through the Diels–Alder reactions. The Diels–Alder cross-linking reaction was carried out between linear polyphosphazene with furan ring side groups and bismaleimide. As the most widely used and studied reversible covalent bonds, Diels–Alder cycloaddition reaction could heal the cracks only need a thermal treatment. But limitations still exist that the hydrogen bonding was weak. And it leads to barely satisfying healing results. The D–A renovating system may consume a lot of time and energy. The reversible photochemical [2+2] cycloaddition has been introduced to self-repairing material by Chung et al. in 2004 [19]. This economical, environmental, and rapid system aroused wide concerns. Therefore, this method could find more broad application scope when it was introduced to polymer materials.

As for the re-healable materials, Hager et al. [5] and Wudl [1] have reviewed the general concepts and fundamentals of re-healable materials. The main methods to prepare re-healable materials in the past decades were summarized in these review literatures. Furthermore, many new systems of re-healable polymers have been reported

by Hager et al. For example, methacrylate copolymers containing terpyridine groups were synthesized, and their polymers could be re-healed by adding metal ions. This polymer showed high re-healing efficiency under mild conditions [20]. Also, they have employed rheological and spectroscopic (FTIR) method to study the re-healing kinetics of Diels–Alder-based copolymers [21]. Detailed information on the re-healing process was reported.

Polyphosphazene was once known as inorganic rubber having a unique structure for its inorganic backbone of alternating phosphorus and nitrogen and substituent organic side chains [22–24]. Due to the biodegradability [25] and the flexible backbone and numerous transformable side chains [26, 27], various analyses were performed on polyphosphazene. However, few research on self-healable polyphosphazene was done.

Allcock et al. [28, 29] once introduced cinnamoyl chloride coumarin/chalcone groups to prepare photo-cross-linkable polyphosphazene. In this work, a new cinnamate molecule with amino group, ethyl 4-aminocinnamate (EA), was introduced to linear polyphosphazenes with one-step reaction to prepare a novel self-healing polyphosphazene via the reversible photochemical [2+2] cycloaddition reaction. The damaged polyphosphazenes could be re-healed almost completely within about half an hour under UV irradiation. The double bonds supplied by EA could be cross-linked readily. Also, the retro- [2+2] cycloaddition occurred under 254 nm, which makes the polyphosphazene to be reprocessed. The structures and properties of the functional polyphosphazenes were studied in detail and fully characterized by UV–vis and SEM.

Experimental section

Materials

Triethylamine (TEA), tetrahydrofuran (THF), *n*-hexane, calcium hydride (CaH₂), petroleum ether (PE), *n*-butylamine, and sodium were purchased from Sinopharm Chemical Reagent Co. Hexachlorocyclotriphosphazene

Table 1 Details of experiments and properties of polyphosphazenes

^a Polymer	PDCP (mmol)	The amount of reactants			^b <i>T</i> _g (°C)	^c <i>T</i> ' _g (°C)	^d <i>T</i> _i (°C)	^e <i>T</i> ' _i (°C)	<i>M</i> _w (g mol ⁻¹)	PDI
		EA/mmol	<i>n</i> -BA/mmol	TEA/mmol						
PBE5	40	4.2	79.8	84	–11	14	210	256	78771	1.92
PBE20	40	16.8	67.2	84	0	19	223	273	116657	1.41
PBE60	40	50.4	33.6	84	–5	31	209	315	145032	1.97

^a Polymer included three polymers, PBE5, PBE20, and PBE60. Here, PBE5, PBE20, and PBE60 represent EA side groups accounted for 5, 20, and 60 % of the total side groups, respectively. ^b*T*_g refers to *T*_g of linear polyphosphazenes. ^c*T*'_g refers to *T*_g of linear polyphosphazenes. ^d*T*_i refers to initial decomposition temperatures of cross-linked polyphosphazenes. ^e*T*'_i refers to initial decomposition temperatures of cross-linked polyphosphazenes

Fig. 1 Synthesis route of linear polyphosphazenes (PBE5: $x/(x+y) = 5\%$, PBE20: $x/(x+y) = 20\%$, PBE60: $x/(x+y) = 60\%$)

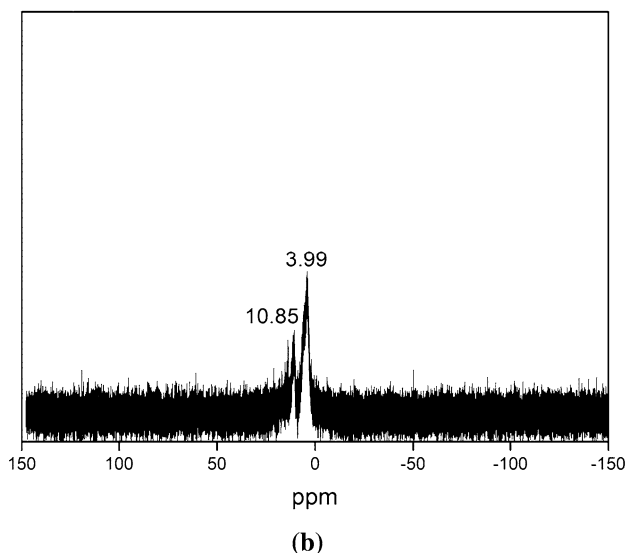
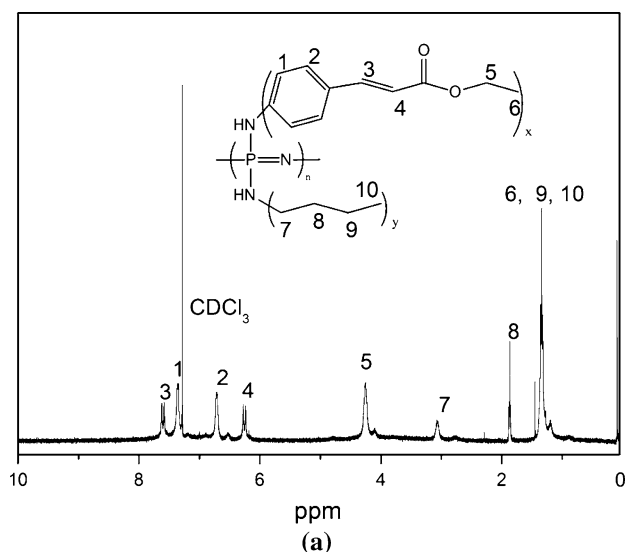
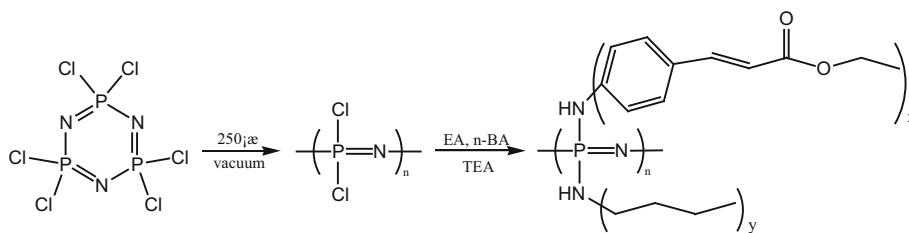


Fig. 2 **a** ^1H -NMR of PBE20, **b** ^{31}P -NMR of PBE20

(HCTP) was purchased from Aladdin Chemical Co. Ltd and purified by re-crystallization from *n*-hexane and subsequent vacuum sublimation at $60\text{ }^\circ\text{C}$. EA was purchased from J&K China Chemical Ltd. Reagents and solvents were used as received without further treatment unless indicated.

Characterizations

^1H -NMR and ^{31}P -NMR spectra were collected on Bruker AVANCE III 400 MHz Digital NMR spectrometer in d_6 - CDCl_3 using TMS and 85% H_3PO_4 as internal standards. Fourier transform infrared (FTIR) spectra were obtained on a Nicolet NEXUS 470 spectrometer. Thermo gravimetric analysis (TGA) measurements were recorded on NETZSCH TG 209F3 apparatus at a heating rate of $10\text{ }^\circ\text{C}/\text{min}$ under N_2 atmosphere. The dried samples were heated from 40 to $600\text{ }^\circ\text{C}$. Dynamic mechanical analysis was conducted on a DMA Q800, TA instrument, from $-80\text{ }^\circ\text{C}$ to $70\text{ }^\circ\text{C}$, at a heating rate of $10\text{ }^\circ\text{C min}^{-1}$. The UV–vis absorption spectra were recorded on a Perkin Elmer lambda 35 UV–vis spectrometer. The micrographs of the surface of the membranes were obtained via field emission scanning electron microscopy (HITACHI, SU8010) under the accelerating voltage of 15.0 kV . UV curing machine is a large-area light source (M-919X) from Newport Co. with a digital exposure controller (M-68950).

Preparation of functional polyphosphazenes

Preparation of poly[di(chloro)phosphazene] (PDCP)

The poly[di(chloro)phosphazene] (PDCP) was prepared using the method described in our previous works [18, 30, 31].

Preparation of poly[(*n*-butylamino) $_x$ (ethyl 4-aminocinnamate) $_y$] phosphazene (PBE)

The above-obtained PDCP was dissolved in dry THF under argon atmosphere. Then EA, *n*-BA, and TEA were added dropwise into the PDCP–THF solution. The mixture was stirred at room temperature for 48 h and then heated to reflux for 24 h. Afterward, the mixture was filtered three times to remove the insoluble salts and precipitated in *n*-hexane twice. Finally, the resultant was dried under a vacuum at $40\text{ }^\circ\text{C}$ for 24 h. All the experimental details are listed in Table 1.

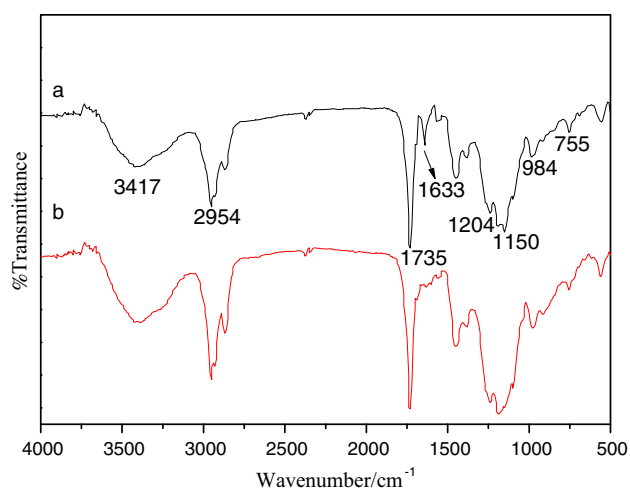


Fig. 3 FTIR of linear and cross-linked PBE: **a** linear PBE20, **b** cross-linked PBE20 (Color figure online)

Preparation of cross-linked PBE membrane

The cross-linked PBE membrane was obtained via solution casting and photo-cross-linking. The PBE–THF transparent solution was poured in a polytetrafluoroethylene (PTFE) slot and covered by a glass slide to slow down the

volatilizing speed. After THF being evaporated completely, the yellowish film was put on a water bag to keep constant temperature at room temperature, and constant distance to the lamp of 30 cm was kept while being exposed to UV (365 nm).

Results and discussion

Structure analysis of linear PBE and cross-linked PBE

As functional side groups, EA was used to substitute C_1 atoms on the chains of PDCP by nucleophilic substitution reaction with TEA as an acid-binding agent. In order to get polyphosphazenes with different ratios of EA side chains, *n*-BA was introduced as an inert substituent to adjust the contents of EA. The synthetic route is shown in Fig. 1. And the parameters of replacement reactions are summarized and shown in Table 1. In particular, PBE5, PBE20, and PBE60 represent EA side groups accounted for 5, 20, and 60 % of the total side groups, respectively, and PBE20 was taken as an example to illustrate the structure of polymer in this work. The linear polyphosphazenes were characterized by $^1\text{H-NMR}$ and $^{31}\text{P-NMR}$. All the peaks of $^1\text{H-NMR}$

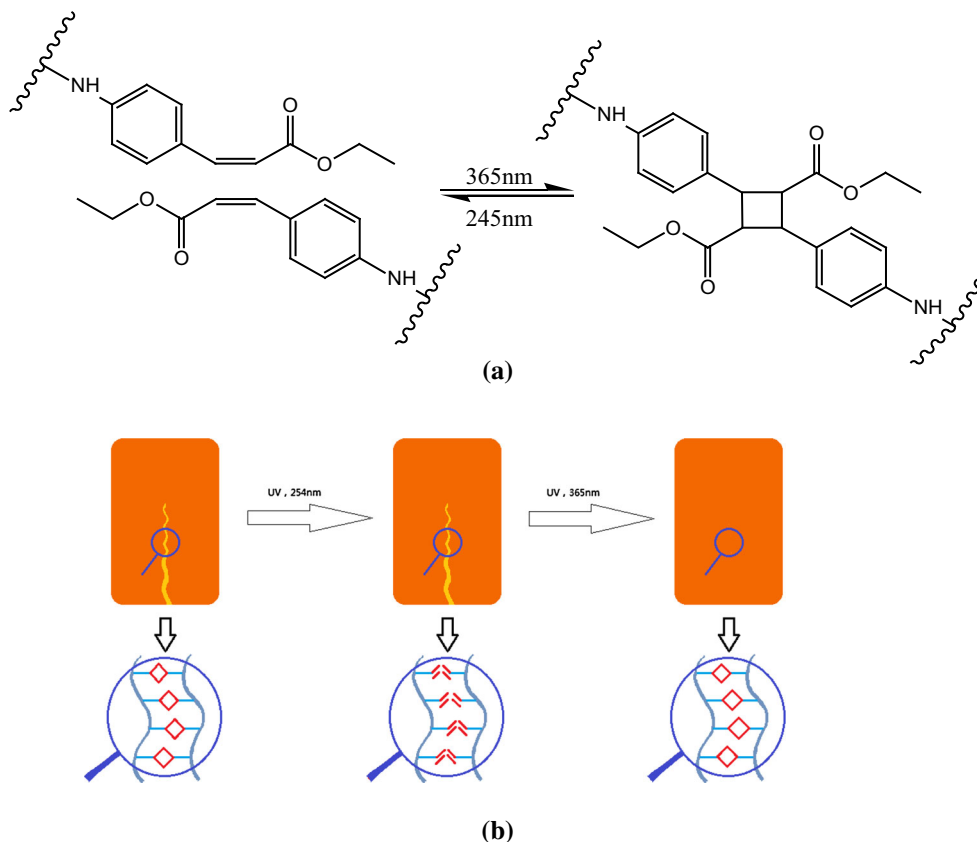


Fig. 4 Schematic diagram of self-repairing: **a** process of photo [2+2] cycloaddition, **b** process of self-healing (Color figure online)

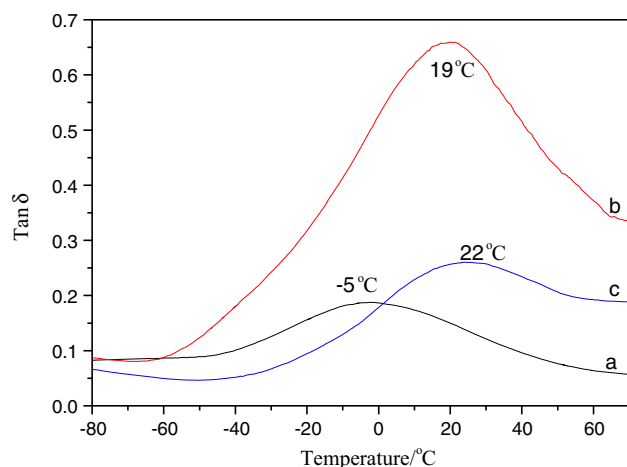


Fig. 5 Dynamic mechanical measurement of $\text{Tan}\delta$: **a** linear PBE20, **b** cross-linked PBE20, **c** reformed cross-linked PBE20 (Color figure online)

shown in Fig. 2a correspond to the hydrogen atoms separately: $-\text{Ph}-\text{CH}=\text{C}-$ at 7.6 ppm, proton on benzene labeled 1 at 7.3 ppm, proton on benzene labeled 2 at 6.7 ppm; and $-\text{Ph}-\text{CH}=\text{C}-$ at 6.2 ppm, $-\text{O}-\text{CH}_2-$ at 4.3 ppm, $\text{N}-\text{CH}_2-$ at 3.1 ppm, the protons on methyl and methylene labeled 6,

9, 10,, at 1.3, 1.4, and 1.5 ppm, respectively. ^{31}P -NMR signals at approximately 10.85 and 3.99 ppm correspond to $\text{P}(\text{EA})_2$ and $\text{P}(\text{n-BA})_2$, respectively (Fig. 2b). The signal of $\text{P}(\text{EA})(\text{n-BA})$ may be between the two signals and covered.

The FTIR spectrum of PBE confirmed the side groups and backbone characteristics of PBE (as shown in Fig. 3, curve a). The $=\text{P}-\text{N}=\text{C}$ bonds were at 755 cm^{-1} , and the strong peaks at 1150 cm^{-1} correspond to the $-\text{P}=\text{N}-$ bonds characteristic absorption of polyphosphazenes, $\text{C}=\text{C}$ bonds were clearly seen at 1633 cm^{-1} , and a strong peak of the $\text{P}-\text{N}-\text{C}$ bonds appeared at 984 cm^{-1} . The absorption at about $1400\text{--}1500\text{ cm}^{-1}$ corresponds to benzene ring. Other absorption peaks at 3417 , 2954 , 1735 , and 1204 cm^{-1} correspond, respectively, to $\text{N}-\text{H}$, $-\text{CH}_2-$, $\text{C}=\text{O}$, and $\text{C}-\text{O}-\text{C}$ breathing.

The data above clearly prove that the functional polyphosphazenes were synthesized successfully, and the mechanism of self-repairing is shown in Fig. 4.

Thermal behavior

The initial decomposition temperatures (T_i) and glass transition temperatures (T_g) of linear and cross-linked

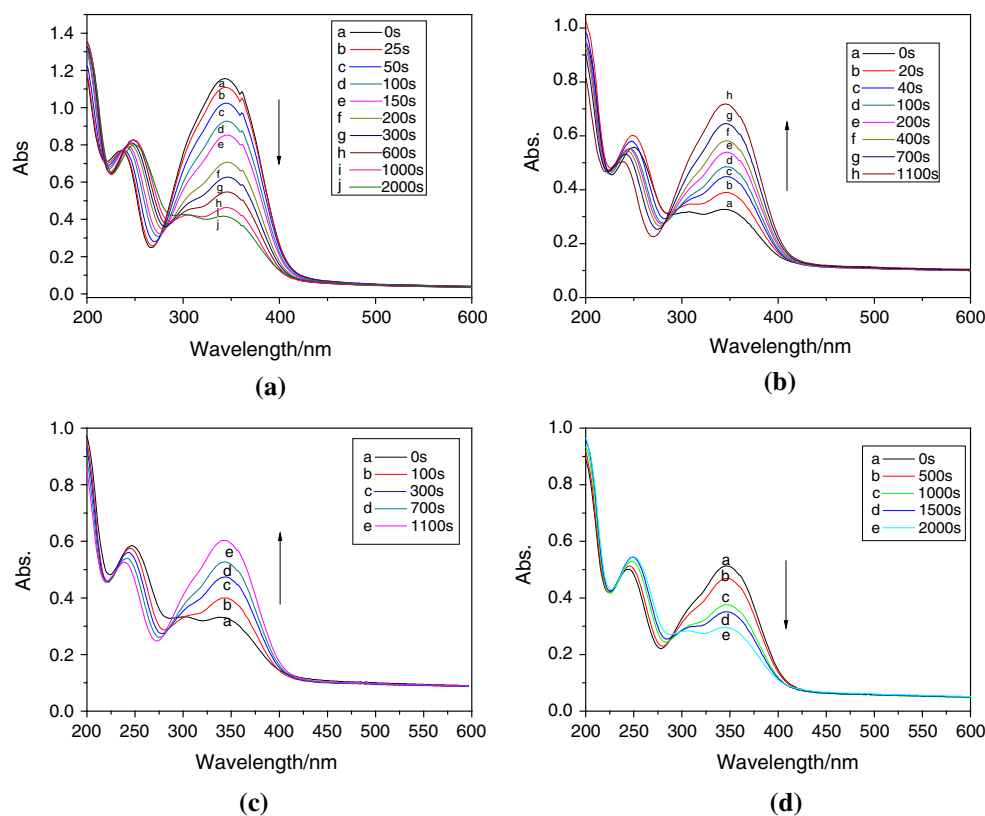


Fig. 6 UV spectroscopy of the progress of reversible photochemical [2+2] cycloaddition: **a** decrease in the absorbance of the progress of the [2+2] cycloaddition reaction at the UV of 365 nm, **b** increase in the absorbance of the progress of the retro-[2+2] cycloaddition reaction at the UV of 245 nm, **c** increase in the absorbance of the

progress of the secondary retro-[2+2] cycloaddition reaction at the UV of 245 nm, **d** decrease in the absorbance of the progress of the secondary [2+2] cycloaddition reaction at the UV of 365 nm. The data were taken from the sample of PBE20 (Color figure online)

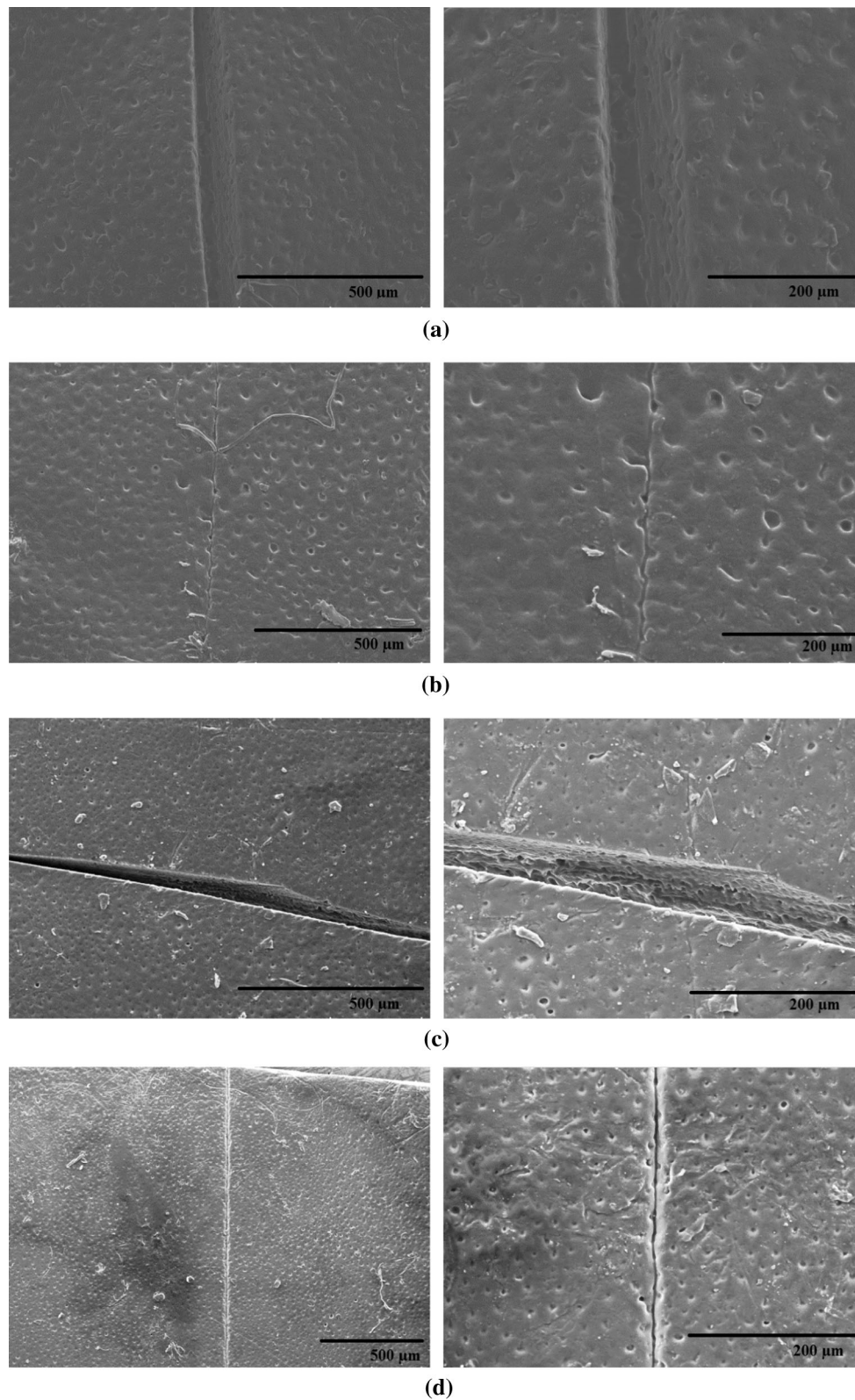


Fig. 7 Photograph of SEM: **a** knife cut on the cross-linked polyphosphazene film surface, **b** scar on the self-repaired film surface, **c** wound of the secondary cut by blade, **d** scar on the secondary self-healed film surface

polyphosphazenes were tested on TGA and DMA, respectively. All the data are listed in Table 1. Comparing the T_i of linear and cross-linked PBE20, it is revealed that the thermal stability could be enhanced by the cross-linking structure. Moreover, conclusion was drawn by the comparison of T_i of cross-linked polyphosphazenes that the thermal stability was also enhanced along with the increasing of cross-linking degree, and the cross-linking degree increased with the ratio of EA. As is shown in Fig. 5, the $\text{Tan}\delta$ versus temperature was plotted. The T_g of the samples could be found at the peak of each curve. It could be found that the uncross-linked sample showed the lowest T_g of $-5\text{ }^\circ\text{C}$ (curve a). Then uncross-linked sample was formed under the UV of 365 nm, and the T_g was increased to $19\text{ }^\circ\text{C}$ (curve b). Afterward, the sample was exposed to the UV of 254 nm to reform to a linear structure and then exposed again to UV of 365 nm to reform to a cross-linked structure. The T_g of the final polymer was recorded (curve c). From curves b and c, it is revealed that there is no obvious change in T_g ($\Delta T_g < 5\text{ }^\circ\text{C}$) for many times. This phenomenon demonstrated that the process of self-repairing did not destroy the structure of the material itself. Even after three circles of [2+2] cycloaddition, the T_g remains unchangeable. It is suggested that this self-healing polyphosphazene could be reprocessed even being undergone cross-linking.

Self-healing of PBE

The [2+2] cycloaddition and retro-cycloaddition reactions, which were the key factors in self-repairability, were tested by FTIR and UV-vis. Membranes with the average thickness of $350\text{ }\mu\text{m}$ were used. As is shown in Fig. 4, the strong absorption of unsaturated double bond at 1641 cm^{-1} disappeared after photo-cycloaddition under the UV of 365 nm. It is suggested that the unsaturated double bonds reacted almost completely. Moreover, the self-healable process (PBE20) was under observation of UV-vis spectrophotometer and SEM. The surface of cross-linked polyphosphazene membrane was cut by blade and then put into a UV curing machine under the UV of 365 nm. The data of UV-vis were recorded continuously until the limit to peak at about 330 nm which was the absorption of unsaturated double bond. The whole process of retro-[2+2] cycloaddition is shown in Fig. 6a and revealed that the cross-linked polyphosphazenes have recovered to linear structure successfully after 1100 s. And the SEM photographs of surface cut are shown in Fig. 7a. Then, the recovered linear polyphosphazene film was exposed to the UV light of 365 nm. The process of [2+2] cycloaddition was continually recorded also by UV-vis. The results reveal that the cross-linking structure was reformed after about 2000 s when the peak at about 330 nm vanished.

Meanwhile, the SEM photographs showed that the surface cut was healed, leaving only a slight scar under SEM.

Then, the scar of the self-healed membrane surface was cut by blade again and treated using the method mentioned above. The process of the secondary self-healing was continually recorded also by UV-vis (Fig. 6c, d). The surface was also characterized by SEM. The results of the UV-vis and SEM (Fig. 7 e, f) showed that the secondary wound could be self-healed again.

The data above fully described the process of self-repairing and proved that these polyphosphazene materials provide a certain capacity of renewing under the stimulus of UV light and could be healed repeatedly.

Conclusions

Self-healing polyphosphazenes were prepared by the photochemical [2+2] cycloaddition reactions of functionalized polyphosphazenes. With the [2+2] cycloaddition reactions between EA groups on polyphosphazenes, the damage could be healed only through a UV stimulus. Moreover, T_i and T_g could be enhanced by the cross-linkage. This method could be employed to prepare functional polyphosphazenes with prolonged life. The used polyphosphazenes could be reprocessed under UV irradiation.

Acknowledgements The authors would like to thank the financial support of NSFC (41240026) and Scientific Research Foundation for the New employees of Southwest University (SWU114110).

References

- Murphy EB, Wudl F (2010) The world of smart healable materials. *Prog Polym Sci* 35:223–251
- Hou CY, Duan YR, Zhang QH, Wang HZ, Li YG (2012) Bio-applicable and electroactive near-infrared laser-triggered self-healing hydrogels based on grapheme networks. *J Mater Chem* 22:14991
- Nosonovsky M, Amano R, Lucci JM, Rohatgi PK (2009) Physical chemistry of self-organization and self-healing in metals. *Phys Chem Chem Phys* 11:9530–9536
- Jackson AC, Bartelt JA, Braun PV (2011) Transparent self-healing polymers based on encapsulated plasticizers in a thermoplastic matrix. *Adv Funct Mater* 21:4705–4711
- Hager MD, Greil P, Leyens C, van der Sybrand Z, Ulrich SS (2010) Self-healing materials. *Adv Mater* 22:5424–5430
- Cho SH, White SR, Braun PV (2009) Self-healing polymer coatings. *Adv Mater* 21:645–649
- Caruso MM, Blaiszik BJ, White SR, Sottos NR, Moore JS (2008) Full recovery of fracture toughness using a nontoxic solvent-based self-healing system. *Adv Funct Mater* 18:1898–1904
- Keller MW, White SR, Sottos NR (2009) A self-healing poly(dimethyl siloxane) elastomer. *Adv Funct Mater* 17:2399–2404
- Hansen CJ, Wu W, Toohey KS, Sottos NR, White SR, Lewis JA (2009) Self-healing materials with interpenetrating microvascular networks. *Adv Mater* 21:4143–4147

10. Cho SH, Andersson HM, White SR, Sottos NR, Braun PV (2011) Accelerated self-healing via ternary interpenetrating microvascular networks. *Adv Funct Mater* 21:4320–4326
11. Xiao DS, Yuan YC, Rong MZ, Zhang MQ (2009) A facile strategy for preparing self-healing polymer composites by incorporation of cationic catalyst-loaded vegetable fibers. *Adv Funct Mater* 19:2289–2296
12. Coope TS, Mayer UFJ, Wass DF, Trask RS, Bon IP (2011) Self-healing of an epoxy resin using scandium (iii) triflate as a catalytic curing agent. *Adv Funct Mater* 21:4624–4631
13. Jin HC, Mangun LA, Griffi S, Moore JS, Sottos NR, White SR (2014) Thermally stable autonomic healing in epoxy using a dual-microcapsule system. *Adv Mater* 26:282–287
14. Barthel MJ, Rudolph T, Teichler A, Paulus RM, Vitz J, Hoepfner S, Hager MD, Schacher FH, Schubert US (2013) Self-healing materials via reversible crosslinking of poly(ethylene oxide)-block-poly(furfuryl glycidyl ether)(PEO-*b*-PFGE) block copolymer films. *Adv Funct Mater* 23:4921–4932
15. Wang C, Liu N, Allen R, Tok JBHY, Wu P, Zhang F, Chen YS, Bao ZN (2013) A rapid and efficient self-healing thermo-reversible elastomer crosslinked with graphene oxide. *Adv Mater* 25:5785–5790
16. Pepels M, Filot I, Klumperman B, Goossens H (2013) Self-healing systems based on disulfide–thiol exchange reactions. *Polym Chem* 4:4955–4965
17. Zeng F, Han Y, Yan ZC, Liu CY, Chen CF (2013) Supramolecular polymer gel with multi stimuli responsive, self-healing and erasable properties generated by host–guest interactions. *Polymer* 54:6929–6935
18. Cheng XJ, Peng C, Zhang DH, Liu SZ, Zhang AQ, Huang H, Lian JS (2013) A facile method for the preparation of thermally remendable cross-linked polyphosphazenes. *J Polym Sci A Polym Chem* 51:1205–1214
19. Chung CM, Roh YS, Cho SY, Kim JG (2004) Crack healing in polymeric materials via photochemical [2+2] cycloaddition. *Chem Mater* 16:3982–3984
20. Bode S, Bose RK, Matthes S, Ehrhardt M, Seifert A, Schacher FH, Paulus RM, Stumpf S, Sandmann B, Vitz J, Winter A, Hoepfner S, Garcia SJ, Spange S, van der ZS, Hager MD, Schubert US (2013) Self-healing metallopolymers based on cadmium bis(terpyridine) complex containing polymer networks. *Polym Chem* 4:4966–4973
21. Bose RK, Kötteritzsch J, Garcia SJ, Hager MD, Schubert US, van der Zwaag S (2014) A rheological and spectroscopic study on the kinetics of self-healing in a single-component Diels-Alder copolymer and its underlying chemical reaction. *J Polym Sci A Polym Chem* 52:1669–1675
22. Allcock HR (2003) Chemistry and applications of polyphosphazenes. Wiley, Hoboken
23. Henke H, Wilfert S, Iturmendi A, Brüggemann O, Teasdale I (2013) Branched polyphosphazenes with controlled dimensions. *J Polym Sci A Polym Chem* 51:4467–4473
24. Weikel AL, Krogman NR, Nguyen NQ, Nair LS, Laurencin CT, Allcock HR (2009) Polyphosphazenes that contain dipeptide side groups: synthesis, characterization, and sensitivity to hydrolysis. *Macromolecules* 42:636–639
25. Greish YE, Benderb JD, Lakshmi S (2005) Low temperature formation of hydroxyapatite-poly(alkyl oxybenzoate)phosphazene composites for biomedical applications. *Biomaterials* 26:1–9
26. Barrett EW, Phelps MVB, Silva RJ, Gaumond RP, Allcock HR (2005) Patterning poly (organophosphazenes) for selective cell adhesion applications. *Biomacromolecules* 6:1689–1697
27. Krogman NR, Weikel AL, Kristhart KA, Nukavarapu SP, Deng M, Nair LS, Laurencin CT, Allcock HR (2009) The influence of side group modification in polyphosphazenes on hydrolysis and cell adhesion of blends with PLGA. *Biomaterials* 30:3035–3041
28. Allcock HR, Cameron CG (1994) Synthesis and characterization of photo-cross-linkable small-molecule and high-polymeric phosphazenes bearing cinnamate groups. *Macromolecules* 27:3125–3130
29. Allcock HR, Cameron CG (1994) Synthesis of photo-cross-linkable chalcone-bearing polyphosphazenes. *Macromolecules* 27:3131–3135
30. Hu L, Zhang AQ, Yu Y, Zheng Z, Du SX, Cheng XJ (2014) Synthesis of hybrid crosslinked polyphosphazenes and investigation of their properties. *Iran Polym J* 23:689–698
31. Hu L, Zhang AQ, Liu K, Lei S, Ou GX, Cheng XJ (2014) A facile method to prepare composite and porous polyphosphazene membranes and investigation of their properties. *RSC Adv* 4:35769–35776